



## *Humulus lupulus* extract rich in xanthohumol improves the clinical course in critically ill COVID-19 patients

Wojciech Dabrowski<sup>a,\*</sup>, Mariusz Gagos<sup>b</sup>, Dorota Siwicka-Gieroba<sup>a</sup>, Mariusz Piechota<sup>c</sup>, Jan Siwiec<sup>d</sup>, Magdalena Bielacz<sup>a</sup>, Katarzyna Kotfis<sup>e</sup>, Andrzej Stepulak<sup>f</sup>, Luiza Grzycka-Kowalczyk<sup>h</sup>, Andrzej Jaroszynski<sup>g</sup>, Manu LNG Malbrain<sup>a</sup>

<sup>a</sup> First Department of Anesthesiology and Intensive Therapy Medical University of Lublin, Lublin, Poland,

<sup>b</sup> Department of Cell Biology, Institute of Biological Sciences, Maria Curie-Skłodowska University, Lublin, Poland,

<sup>c</sup> Department of Anesthesiology and Intensive Therapy, Centre for Artificial Extracorporeal Kidney and Liver Support, Dr. W. Bieganski Regional Specialist Hospital, Łódź, Poland,

<sup>d</sup> Department of Pneumology, Oncology and Allergology Medical University of Lublin, Poland,

<sup>e</sup> Department of Anesthesiology, Intensive Therapy and Acute Intoxications, Pomeranian Medical University, Szczecin, Poland,

<sup>f</sup> Department of Biochemistry and Molecular Biology, Medical University of Lublin, Poland,

<sup>g</sup> Collegium Medicum, Jan Kochanowski University of Kielce, Poland,

<sup>h</sup> First Department of Medical Radiology, Medical University of Lublin, Poland

### ARTICLE INFO

#### Keywords:

Xanthohumol  
COVID-19  
Coronavirus  
Critically ill  
Inflammatory response  
Neutrophil-to-lymphocyte ratio  
Mortality

### ABSTRACT

**Background:** The systemic inflammatory response following severe COVID-19 is associated with poor outcomes. Several anti-inflammatory medications have been studied in COVID-19 patients. Xanthohumol (Xn), a natural extract from hop cones, possesses strong anti-inflammatory and antioxidative properties. The aim of this study was to analyze the effect of Xn on the inflammatory response and the clinical outcome of COVID-19 patients.

**Methods:** Adult patients treated for acute respiratory failure (PaO<sub>2</sub>/FiO<sub>2</sub> less than 150) were studied. Patients were randomized into two groups: Xn – patients receiving adjuvant treatment with Xn at a daily dose of 4.5 mg/kg body weight for 7 days, and C – controls. Observations were performed at four time points: immediately after admission to the ICU and on the 3rd, 5th, and 7th days of treatment. The inflammatory response was assessed based on the plasma IL-6 concentration, neutrophil-to-lymphocyte ratio (NLR), platelet-to-lymphocyte ratio (PLR), C-reactive protein (CRP) and D-dimer levels. The mortality rate was determined 28 days after admission to the ICU.

**Results:** Seventy-two patients were eligible for the study, and 50 were included in the final analysis. The mortality rate was significantly lower and the clinical course was shorter in the Xn group than in the control group (20% vs. 48%,  $p < 0.05$ , and  $9 \pm 3$  days vs.  $22 \pm 8$  days,  $p < 0.001$ ). Treatment with Xn decreased the plasma IL-6 concentration ( $p < 0.01$ ), D-dimer levels ( $p < 0.05$ ) and NLR ( $p < 0.01$ ) more significantly than standard treatment alone.

**Conclusion:** Adjuvant therapy with Xn appears to be a promising anti-inflammatory treatment in COVID-19 patients.

**Abbreviations:** ACE-2, Angiotensin converting enzyme 2; ALIC, Absolute lymphocyte count; APACHE II, Acute Physiology and Chronic Health Evaluation II; APTT, Activated partial thromboplastin time; CoV-2, Coronavirus-2; CI, Cardiac index; CO, Cardiac output; CRP, C-reactive protein; CT, Computed tomography; DGAT, Diacylglycerol acyltransferase; FXR, Farnesoid X receptor; HMGB1, High-mobility group box 1 protein; HR, Heart rate; ICU, Intensive care unit; iNOS, Inducible nitric oxide synthase; IXn, Isoxanthohumol; MAP, Mean arterial pressure; NADPH, Nicotinamide adenine dinucleotide phosphate; NLR, Neutrophil-to-lymphocyte ratio; ORI, Oxygen reserve index; PLR, Platelet-to-lymphocyte ratio; PRRSV, Porcine reproductive and respiratory syndrome virus; ROS, Reactive oxygen species; SAPS, Simplified Acute Physiology Score; SARS-CoV-2, Severe Acute Respiratory Syndrome (induced by) Coronavirus-2; SOFA, Sequential Organ Failure Assessment Score; SpO<sub>2</sub>, Peripheral saturation; SrO<sub>2</sub>, Cerebral tissue oxygen saturation; SVV, Stroke volume variation; WBC, White blood cells; Xn, Xanthohumol.

\* Correspondence to: First Department of Anesthesiology and Intensive Therapy Medical University of Lublin, Jaczewskiego Street 8, 20-954 Lublin, Poland.

E-mail addresses: [w.dabrowski5@yahoo.com](mailto:w.dabrowski5@yahoo.com), [wojciech.dabrowski@umlub.pl](mailto:wojciech.dabrowski@umlub.pl) (W. Dabrowski).

<https://doi.org/10.1016/j.bioph.2022.114082>

Received 3 September 2022; Received in revised form 22 November 2022; Accepted 2 December 2022

0753-3322/© 2022 The Author(s). Published by Elsevier Masson SAS. This is an open access article under the CC BY-NC-ND license (<http://creativecommons.org/licenses/by-nc-nd/4.0/>).

## 1. Introduction

Since December 2019, when a new type of severe acute respiratory syndrome coronavirus (SARS-CoV-2) was described, many studies have been performed to identify an effective treatment to alleviate its signs and symptoms. This infection is caused by  $\beta$ -coronavirus 2 (CoV-2) and is associated with multiorgan dysfunction resulting mainly from endothelial damage complicated by massive inflammatory response syndrome [1–4]. Coronavirus-induced symptoms are referred to as COVID-19.

Several studies on COVID-19 documented a strong relationship between the severity of the clinical condition and the degree of inflammatory response to viral infection [5–8]. Immune dysregulation is a trigger for cytokine storms. An increase in the release of inflammatory cytokines, especially interleukin-6 (IL-6), associated with T-cell lymphopenia is correlated with poor outcomes and death [5,6,8]. A rapid increase in the inflammatory response is associated with the uncontrolled production of reactive oxygen species and free radicals, which significantly impair cellular metabolism [9,10]. Several authors have studied the efficiency of anti-inflammatory and antioxidant treatment to reduce COVID-19-related complications and death [5,9–17]. Interestingly, natural compounds have also been suggested as effective adjuvants in COVID-19 therapy [18,19]. These compounds possess different anti-COVID-19 activities. Some of these compounds block IL-6 release, which could reduce the need for mechanical ventilation and thus also admission to the intensive care unit (ICU) [13–15]. Other compounds directly inhibit viral replication by binding to specific receptors [20,21]. Interestingly, some of these compounds have similar chemical structures. In silico studies suggested a high efficiency of naturally occurring prenylated chalcones for treating coronavirus infection [15,22,23].

Xanthohumol (Xn) is a prenylated chalcone (Fig. 1) that can be extracted from female inflorescences of hop cones (*Humulus lupulus*). Increasing numbers of studies have documented the immunomodulatory properties of Xn [24–26]. Xanthohumol inhibits proinflammatory pathways via inhibition of farnesoid X receptor (FXR) activity and NF- $\kappa$ B-dependent inhibition of proinflammatory gene expression, such as IL-1 $\beta$ , IL-6, IL-8, IL-12p70, TNF $\alpha$ , and interferon  $\gamma$  [23–26]. Experimental studies have documented a strong effect of Xn against many DNA and RNA viruses, such as herpes simplex virus types 1 and 2, cytomegaloviruses, and porcine reproductive and respiratory syndrome virus (PRRSV) [22,25–28].

Interestingly, PRRSV infection is similar to the course of coronavirus infection, with the main symptoms consisting of high fever, significant morbidity, and severe respiratory disease resulting in high mortality. In vivo experiments showed that PRRSV-infected piglets treated with Xn at a dose of 20 mg/kg exhibited only moderate clinical signs and low viral loads, whereas 25 mg/kg Xn practically eliminated all clinical symptoms [28]. Another experimental study documented that Xn inhibited many viral diseases, including SARS-CoV-2 and other fatal diseases

caused by alpha- or beta-coronavirus [29]. Notably, Xn is safe and well tolerated in healthy humans and is available as a dietary supplement. Based on its antiviral and anti-inflammatory properties, we hypothesized that the administration of Xn could improve the clinical course and outcome in critically ill COVID-19 patients requiring mechanical ventilation.

Therefore, the aim of this study was to analyze the effect of Xn supplementation on the clinical course, inflammatory response, and outcome in patients admitted to the ICU due to COVID-related acute respiratory failure with an oxygenation index (PaO<sub>2</sub>/FiO<sub>2</sub>) less than 150.

## 2. Patients and methods

### 2.1. Ethical considerations

This prospective, observational study was conducted in accordance with the Declaration of Helsinki and applicable regulatory requirements. The local Institutional Review Board and the Bioethics Committee of the Medical University in Lublin, Poland approved the protocol (KE-0254/201/2020). Written informed consent was obtained from all patients just after admission to the ICU prior to randomization. Additionally, the patient's legal representatives were informed about the main purpose of this study. The present study is registered at ClinicalTrials.gov (<http://www.clinicaltrials.gov>) with the unique identifier NCT05463393.

### 2.2. Study drug treatment

All patients were treated following current guidelines at the time of admission. After admission to the hospital, remdesivir (Veklury, Ireland) was administered at an initial dose of 200 mg/day followed by 100 mg/day for 5–7 days. Additionally, vitamin D3 at a dose of 4000 U per day was supplemented in all patients. Corticosteroid therapy with dexamethasone (Dexaven, GmbH Arzneimittel, Germany) at a dose of 8 mg per day for 10 days and anticoagulant therapy with enoxaparin (Clexane, Sanofi-Aventis, France) were started upon admission to the ICU. All patients received a continuous infusion of insulin to maintain plasma glucose concentrations between 100 and 160 mg/dL.

Patients who were included in the present study received additional treatment with Xn or normal saline. Patients were randomized in a double-blind, placebo-controlled fashion into two groups using sealed envelopes. Group Xn included patients who received an extract from *Humulus lupulus* L rich in xanthohumol (Hop-RXn™, BioActive-Tech Ltd., Lublin, Poland; <http://xanthohumol.com.pl/>) as adjuvant therapy, and Group C included patients who received 0.9% NaCl and formed the control group. Based on its pharmacokinetics and bioactivity, Xn was administered enterally three times a day every 8 h at a dose of 1.5 mg/kg body weight (4.5 mg/kg body weight/day) for 7 days [30]. The first dose of Xn was administered within 4 h after admission to the ICU. In the control group, 3 mL of 0.9% NaCl was administered enterally three times a day.

### 2.3. Monitoring

In all patients, systolic diastolic and mean arterial blood pressure (MAP), heart rate (HR), and expiratory CO<sub>2</sub> tension were monitored continuously. Additionally, hemodynamic variables, such as cardiac output/index (CO/CI), stroke volume variation (SVV), systemic vascular resistance index (SVRI), and central venous pressure (CVP), were monitored using the EV 1000 platform (Edwards Lifescience, Irvine, CA, USA). Masimo Root monitor (USA) with SEDLine was used for continuous measurement of regional cerebral oxygen saturation (SrO<sub>2</sub>), frontotemporal electroencephalography, peripheral oxygen saturation (SpO<sub>2</sub>) with hemoglobin level, and oxygen reserve index (ORI). Fluid administration with balanced crystalloids and vasopressors (norepinephrine) was titrated to obtain a MAP higher than 65 mmHg.

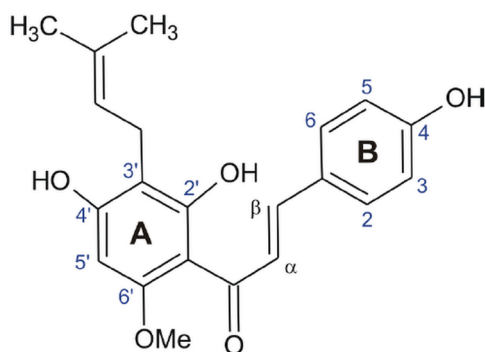


Fig. 1. Chemical structure of xanthohumol (2',4',4-trihydroxy-6'-methoxy-3-(3methyl-but-2-en-1-yl) with atom numbering.

## 2.4. Patient selection and inclusion criteria

This study was performed between October 2020 and January 2021. Adult patients aged 18 years or older admitted to the ICU who were treated for severe COVID-19 with acute respiratory failure ( $\text{PaO}_2/\text{FiO}_2$  below 150) due to bilateral and multifocal ground-glass opacities involving greater than half of the lungs were included in this study. Quantitative computed tomography (CT) with thoracic VCAR software and the parenchymal analysis option were used to assess the degree of parenchymal impairment. Patients who were treated for COVID-19 for more than one week were excluded. Other exclusion criteria were chronic renal failure, history of illness affecting the human immune system (modulated immune system, such as transplant patients), and/or diseases causing prolonged inflammatory responses such as malignancies, rheumatologic diseases, and chronic inflammatory disease. Pregnant or lactating women were also excluded. Patients who did not respond to the prone ventilation strategy were screened for eligibility for extracorporeal oxygenation (ECMO) and were excluded from this study. Patients who died within 7 days were also excluded due to incomplete data.

## 2.5. Biochemical analysis

Routine biochemical examination with full blood count and morphology, including erythrocyte, platelet, leukocyte, neutrophil and lymphocyte counts, serum interleukin 6 (IL-6) concentration, C-reactive protein (CRP) and D-dimers, were performed at the laboratory of University Hospital No. 4 in Lublin, Poland using commercial reagents. Arterial blood gas analysis was performed a minimum of 4–6 times per day using GEM 5000 (Werfen, Barcelona, Spain).

## 2.6. Pulmonary disease evaluation

The ventilator settings were determined in accordance with the results of the blood gas examination, and respiratory insufficiency was assessed by calculating the  $\text{PaO}_2$ -to- $\text{FiO}_2$  ratio ( $\text{PaO}_2/\text{FiO}_2$ ). Patients with  $\text{PaO}_2/\text{FiO}_2$  less than 100 were placed into the prone position in accordance with the local protocol [31]. A high-resolution computed tomography (CT) technique with artificial intelligence software (Thoracic VCAR software with Parenchymal Analysis, GE Healthcare, USA) was used to assess the severity and quantitatively measure lung injury. In all participants, CT was performed immediately before admission to the ICU. A control CT was performed 2–3 days after extubation or immediately after discharge from the COVID zone in the ICU.

## 2.7. Study protocol, measured variables and outcomes

Observations were performed at four time points: 1) immediately after admission to the ICU (baseline), 2) 3 days after admission to the ICU, 3) on the 5th day of treatment and 4) on the 7th day of treatment. The degree of the inflammatory response was measured by NLR, PLR, D-dimer, and plasma IL-6 concentration. The following formulas were used for the calculation of NLR and PLR [32,33]:

- NLR: the number of neutrophils divided by the number of lymphocytes,
- PLR: the number of platelets divided by the number of lymphocytes.

The  $\text{PaO}_2/\text{FiO}_2$  ratio was calculated as the ratio between the oxygen tension obtained from routine blood gas analysis and the fraction of inhaled oxygen ( $\text{FiO}_2$ ). The primary outcome was mortality rates, which were determined at 7 and 28 days after admission to the ICU. The secondary outcomes were the dynamics and evolution of the inflammatory parameters and the evolution of CT imaging.

## 2.8. Statistical analysis

Statistical analysis was performed using Statistica 13.1 software (StatSoft, USA). Means and standard deviations (SD) were calculated for normally distributed variables, whereas non-Gaussian distributed variables were presented as medians and interquartile ranges. The Kolmogorov–Smirnov test was used to analyze the normality of the data distribution. Categorical variables were compared using the  $\chi^2$  and Fisher exact tests, and Yates correction was applied. The value at ICU admission was regarded as the baseline. Unpaired Student's *t*-test was used to analyze variables with a normal distribution. Nonparametric data were statistically analyzed using the Wilcoxon signed-rank test and the Kruskal–Wallis test. Additionally, the Pearson test was used for the analysis of any correlations among normally distributed variables, whereas Spearman's rank test was used for interpoint and intergroup comparisons for variables with a non-Gaussian distribution. Kaplan–Meier estimation with a log-rank test was performed for survival probability analysis. A value of  $p < 0.05$  was considered significant, and the power of the statistical test ( $1 - \beta$ ) was calculated using G\*Power 3.1 software.

## 3. Results

### 3.1. Study population

Seventy-two critically ill adult patients treated for COVID-19 with severe respiratory failure were included in the present study. A total of 22 patients were excluded from the final analysis: 11 were excluded because informed consent could not be obtained, and 4 died within 7 days with incomplete data. Additionally, seven patients were excluded due to incomplete data or consent withdrawal after recovery. Finally, fifty patients (18 women and 32 men) aged 22–83 years (mean  $58 \pm 17$ ) were studied. Twenty-five patients were randomly assigned to the Xn group and were treated with Xn, and 25 received 0.9% NaCl and were allocated to the control group. The relevant demographic data and comorbidities are presented in Table 1.

### 3.2. Primary endpoints

Overall mortality was 34%. Seventeen patients died between Days 7

**Table 1**

Baseline demographic data and comorbidities. NS – not statistically significant. \*  $p < 0.05$  – differences in the SOFA score from the baseline, S \* \*  $p < 0.01$  – differences in the SOFA score after the exclusion of patients who died between Days 7 and 28 (Student's *t*-test).

	Xn group	Control group	p value
Female/Male	8/17	11/14	NS
Mean BMI ( $\text{kg}/\text{m}^2$ )	$29.95 \pm 5.34$	$31.09 \pm 6.81$	NS
Comorbidities			
Diabetes	16	13	NS
Hypertension	21	23	NS
Coronary disease	12	9	NS
Cardiac arrhythmia	6	4	NS
Asthma	2	0	NS
Thyroid disease	0	1	NS
Gout	3	0	NS
Immunology disorders	1	0	NS
Duration of mechanical ventilation (days)	$9 \pm 3$ days	$22 \pm 8$ days	$p < 0.001$
Septic complications	0	9	$p < 0.01$
Baseline APACHE II score	$13.6 \pm 3.7$	$12.8 \pm 4.1$	NS
Baseline SAPS II score	$35.7 \pm 5.4$	$34.6 \pm 4.8$	NS
SOFA			
Baseline	$5.5 \pm 3$	$5.3 \pm 3.7$	NS
3rd day	$4.9 \pm 2.4$	$5.3 \pm 2$	NS
5th day	$4.7 \pm 3.1$	$5.2 \pm 3.1$	NS
7th day	$3.5 \pm 2.8$ *	$4.4 \pm 3.1$	NS (S **)

and 28 of treatment: 5 (20%) in the Xn group and 12 (48%) in the control group ( $\chi^2 = 5.56$ ,  $p < 0.05$  and  $\chi^2$  with Yates correction = 4.25 and  $p < 0.05$ , Fig. 2). All patients treated with Xn who survived were discharged from the ICU to the pulmonology or rehabilitation ward and then discharged home in good clinical condition. In the control group that did not receive Xn, none of the patients were discharged directly home. These patients were discharged to another pulmonology hospital followed by another hospital, and their outcomes could not be determined.

### 3.3. Changes in inflammatory markers

The mean baseline value of NLR was  $20.8 \pm 16$  in all participants and was comparable in both groups ( $21.5 \pm 14.2$  vs.  $20.2 \pm 17.6$  in the Xn treated and control groups, respectively). Treatment with Xn resulted in a nearly 5-fold significant reduction in NLR at Day 7 compared with baseline. In contrast, no significant NLR decrease was observed in the control group (Table 2). In patients who survived, the NLR decreased on the 3rd and 7th days of treatment with Xn and on Day 7 in the control group (Fig. 3).

The platelet-to-lymphocyte ratio decreased on the 3rd and 7th days of treatment in the Xn group and on the 5th and 7th days in the control group (Table 2). Changes in both groups were comparable, and no significant differences were noted.

The mean baseline value of the plasma IL-6 concentration was  $279.1 \pm 380.1$  pg/mL in all patients. IL-6 levels were comparable in both groups ( $298.4 \pm 453.5$  pg/mL vs.  $256.7 \pm 337.5$  pg/mL in the Xn-treated and control groups, respectively). Treatment with Xn reduced plasma IL-6 concentrations on the 3rd and 7th days, whereas these values were reduced on the 5th and 7th days in the control group (Table 2). In patients who survived, the plasma IL-6 concentration decreased on Days 3, 5, and 7 in both groups. The decrease in plasma IL-6 concentration was more pronounced in the Xn group (Fig. 4).

In both groups, D-dimer levels decreased on the 3rd, 5<sup>th</sup>, and 7th days; however, treatment with Xn resulted in a more pronounced reduction compared to the control group (Table 2). In patients who survived, D-dimers decreased in both studied groups, but their concentrations were significantly lower in patients treated with Xn on the 3rd and 7th days ( $p < 0.05$ ).

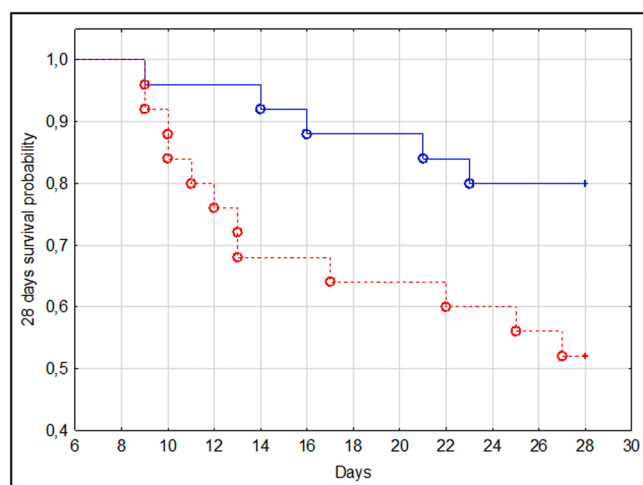


Fig. 2. The Kaplan–Meier estimation with a log-rank test for the 28-day probability of survival in patients receiving adjuvant therapy with xanthohumol at a daily dose of 4.5 mg per kg body weight (— Xn group) and patients who did not receive adjuvant therapy (--- Control group).

### 3.4. Changes in CT lung scans and gas exchanges ( $PaO_2/FiO_2$ )

In all patients, a CT examination of the lung showed massive bilateral and multifocal ground-glass opacities (Table 3). A significant improvement in CT lung scans was noted in patients treated with Xn (Fig. 5), whereas only a slight improvement was noted in patients treated with placebo (Fig. 6). Additionally, mechanical ventilation was completed within 7 days in 14 Xn patients, and 6 patients required mechanical ventilation/support for more than 7 days. None of these patients required a tracheostomy. In the control group, mechanical ventilation was completed within 7 days in only 4 patients, and 8 of them required percutaneous tracheostomy due to the necessity of prolonged mechanical ventilation for up to 14 days.  $PaO_2/FiO_2$  decreased in both groups; however, the changes were more pronounced in the Xn group (Table 2).

## 4. Discussion

In the present study, we documented that treatment with Xn significantly reduced the severity of the inflammatory response, as reflected by the plasma IL-6 concentration and NLCR, improved patient outcomes and reduced the mortality rate. Additionally, Xn at a daily dose of 4.5 mg/kg body weight improved the oxygenation index and reduced the length of mechanical ventilation. The mechanism responsible for these phenomena seems to be complex and pleiotropic.

### 4.1. Presumed pathophysiological mechanisms

Xanthohumol is the most abundant prenylated flavonoid in hops. Beer is the most important dietary source of Xn and other related prenylflavonoids. Admittedly, the brewing process induces thermal isomerization of Xn to isoxanthohumol (IXn), but Xn can be converted into IXn in the stomach [34,35]. An in vitro study showed that both forms could be biotransformed by human liver microsomes into glucuronides, hydroxylated metabolites, and cyclic dehydrometabolites [30,35,36]. The bioavailability of Xn is dose-dependent and it increases linearly with an increasing oral dose [30]. Xn has strong antioxidant and anti-inflammatory properties and protects cells from injury induced by upregulated angiotensin-2 activation [23–26,37,38].

An experimental study showed that angiotensin-2 stimulates the production of reactive oxygen species (ROS) via the activation of nicotinamide adenine dinucleotide phosphate (NADPH) oxidase, and Xn and its major bioactive metabolite IXn strongly inhibit this process, preventing oxidative-related endothelial injury [37,39]. It was previously shown that Xn inhibits the viral-encoded cysteine protease (the main protease of CoV-2) in a dose-dependent manner [29]. Importantly, this protease is necessary for viral replication. Another reported pathomechanism is based on a reduction in the intensity of viral replication related to the inhibition of diacylglycerol acyltransferase (DGAT) [20]. Massive viral replication is associated with metabolic cell damage, and the rapid upregulation of lipid biosynthesis, particularly triacylglycerol, plays a crucial role in this process. The last step in triacylglycerol synthesis is catalyzed by DGAT, the inhibition of which reduces the availability of fuel for viral replication. Xanthohumol strongly inhibits DGAT activity in a dose-dependent manner, and its antiviral effect has been noted in cardiomyocytes and type II alveolar epithelial cells – the major portal of CoV-2 infection [20]. Interestingly, Xn has the most potent activity among all chalcones extracted from *Humulus lupulus* [38]. In the present study, we observed relatively quick improvements in blood oxygenation and CT-lung imaging after only 7 days of treatment with Xn. Therefore, we can speculate that the use of Xn at a dose of 4.5 mg/kg body weight may be a safe and effective adjuvant therapy in severe COVID-19 patients.

### 4.2. Anti-inflammatory properties

The therapeutic effect of Xn can also be explained by its anti-

**Table 2**

Changes in the selected biochemical variables and the PaO<sub>2</sub>/FiO<sub>2</sub> ratio in the two study populations (neutrophil-to-lymphocyte ratio (NLR), plasma IL-6 concentration, C-reactive protein (CRP), platelet-to-lymphocyte ratio (PLR), absolute lymphocyte count (ALC)), and white blood cell count (WBC). Data are presented as medians and quartiles 1 and 3. \* p < 0.05, p < 0.01, \*\*\* p < 0.001 – difference compared to baseline. ‡ p < 0.05, ‡‡‡ p < 0.01 – the difference between the Xn and control groups.

	Xn group				Control group			
	Baseline	Day 3	Day 5	Day 7	Baseline	Day 3	Day 5	Day 7
WBC	10.2 [7.9; 14.12]	13.8 ** [10.13; 17.9]	12.5 ** [9.86; 15.46]	10 [9.75; 14.5]	10.42 [6.9; 14.62]	11.4 [8.92; 13.98]	12.85 * [9.44; 15.85]	12.4 [8.55; 16.13]
ALC	0.4 [0.33; 0.64]	0.85 * **‡ [0.72; 1.38]	1.1 ** [0.4; 1.6]	1.91 ** [0.79; 1.96]	0.54 [0.4; 0.79]	0.7 [0.57; 0.93]	1.05 [0.89; 1.24]	1.2 ** * [0.95; 1.4]
NLR	23.64 [13.45; 27.71]	12.61 [6.49; 21.29]	7.75 [5.44; 31.34]	4.28 * [3.96; 22.41]	16.44 [8.08; 23.75]	12.30 [9.4; 19.07]	10.48 [7.6; 19.9]	7.03 [5.67; 14.79]
IL-6	105.5 [40.4; 406.8]	33.8 * ** [13.52; 129.1]	8.4 * ‡‡ [4.81; 56]	29.1 * **‡‡ [5.65; 40.41]	165.1 [70.48; 287.17]	146.2 [34.1; 283.7]	124.9 * [53.8; 200.1]	109.6 * [52.2; 168.4]
CRP	98.2 [18.95; 151.14]	58.96 ** [9.13; 77.71]	38.2 * [4.8; 51.19]	38.32 [5.49; 69.96]	92.4 [27.25; 154.55]	57.83 * [38.8; 94.7]	48.09 [24.8; 94.4]	41.3 [21.8; 58.3]
D-dimers	4907 [782.5; 23549]	2429 ** [794.7; 4102]	1802.5 ** [910; 2237]	723 * **‡ [505.25; 1894]	4675.5 [1325.8; 11385]	3459.5 * [1765; 8289.3]	1955 * [916.8; 4509]	2147 * [1021; 3846]
PLR	762 [409; 800.5]	316.5 * [220.45; 356.4]	290 [197.77; 513.5]	178.7 * [155.3; 307.4]	457.5 [350.9; 741.67]	374.4 [283.5; 556.6]	340 [219.8; 445]	267.4 * ** [204.1; 373.5]
PaO <sub>2</sub> /FiO <sub>2</sub>	58 [52.25; 98.16]	95.12 ** [82.18; 142.42]	98.75 ** [78.68; 185.4]	148.5 * **‡ [119.6; 295.27]	59.9 [50.9; 87.8]	112.8 * ** [89.2; 128.9]	119.1 * ** [88.7; 177.8]	125.4 * ** [111; 146.45]

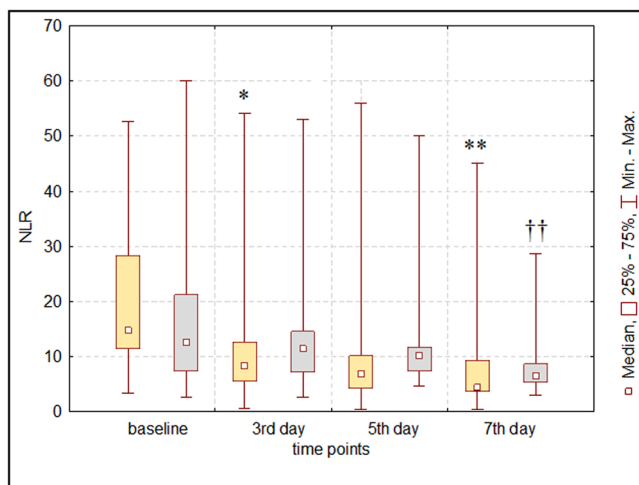


**Fig. 3.** Evolution of the neutrophil-to-lymphocyte ratio (NLR) in survivors receiving xanthohumol (■ - Xn group, n = 20) as an adjuvant therapy compared to those treated with placebo (■ - control group, n = 13). \* p < 0.05, \*\* p < 0.01 – differences from the baseline in the Xn group, †† p < 0.01 – differences from the baseline in the control group. The power of the statistical analysis was > 0.8.

inflammatory properties. We noted a significantly lower IL-6 concentration and NLR in patients treated with Xn. Rapid and massive production of proinflammatory cytokines, particularly IL-6, is associated with the severity of COVID-19. In the present study, the plasma IL-6 concentration upon admission was 100-fold higher than normal, and the addition of Xn to the treatment regimen resulted in a rapid and significant decrease in its concentration. Several studies documented the strong anti-inflammatory properties of Xn with a reduction in proinflammatory cytokines and the number of macrophages in injured tissues [24,40,41]. Administration of Xn reduced plasma IL-6 levels by approximately 80% [42]. An animal study showed that Xn effectively reduced tumor necrosis factor-alpha (TNF-α), IL-6, and IL-1β secretion and suppressed high-mobility group box 1 protein (HMGB1) and inducible nitric oxide synthase (iNOS) expression [40]. A decrease in the production and release of proinflammatory cytokines is associated with the suppression of nuclear factor-kappa B (NF-κB), which inhibits T-cell proliferation [29,40,41]. Interestingly, anatomopathological examination of animal lungs revealed significantly lower neutrophil infiltration in injured lungs, and lung damage was markedly reduced in animals

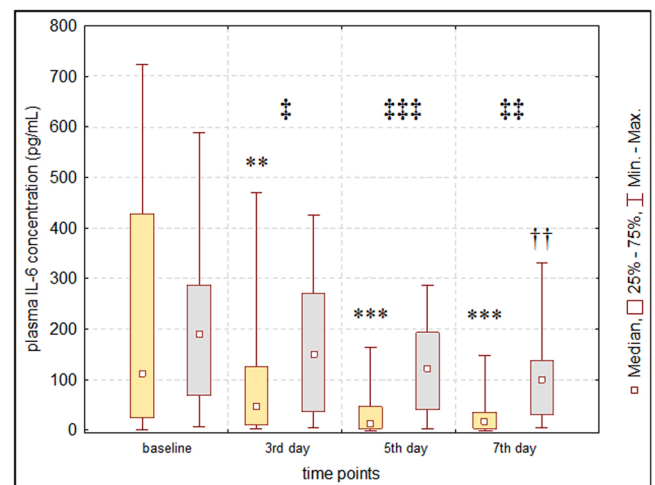


**Fig. 4.** Evolution of the plasma IL-6 concentration in survivors receiving xanthohumol (■ - Xn group, n = 20) as adjuvant therapy and those treated with placebo (■ - control group, n = 13). \*\* p < 0.01, \*\*\* p < 0.001 – differences from the baseline in the Xn group, †† p < 0.01 – differences from the baseline in the control group. ‡ p < 0.05, ‡‡ p < 0.01, ‡‡‡ p < 0.001 – difference between the Xn and control groups. The power of the statistical analysis was > 0.8.

treated with Xn compared to those treated with remdesivir [20,41]. In the present study, CT scans also showed markedly fewer consolidations and bilateral diffuse mixed densities of the lung in patients treated with Xn compared to controls. All of our patients tolerated Xn well, and none of them had adverse effects. Therefore, we suggest adding Xn as an adjuvant to standard therapy in COVID-19 patients.

The neutrophil-lymphocyte count ratio is frequently used as a marker of the severity of inflammation and outcome [43–47]. Elevated NLR values predict poor outcomes in patients treated for traumatic brain injury [43], mesenteric ischemia [44], or sepsis [45]. Importantly, NLR has also been proposed as a sensitive marker of endothelial dysfunction following viral infection [46]. Progressive endothelial damage following viral infection, including CoV-2, induces massive glycocalyx injury, leading to endothelial inflammation with uncontrolled neutrophil activation, vasoconstriction, and coagulation disorders [3,4,47]. Anatomopathological examination of lungs from patients with COVID-19 showed the presence of viral inclusions and massive inflammation in endothelial cells [48–50]. The virus binds to the angiotensin-converting enzyme 2

**Table 3**

Evolution of lung injury measured with high-resolution computed tomography (CT) combined with artificial intelligence software with the percentage of the pulmonary parenchyma and affected automatic detection of pathology (emphysema, normal parenchyma, ground glass opacity, and consolidation). Percentages are expressed as the mean with standard deviation (SD). Baseline – CT performed immediately before admission to the ICU. \*\*  $p < 0.01$ , \*\*\*  $p < 0.001$  – changes between the baseline and control lung pathologies assessed by artificial intelligence software, †  $p < 0.05$ , ††  $p < 0.001$  – differences between lung pathologies observed in the Xn and control groups.

	Xn group		Control group	
	Baseline CT	Control CT	Baseline CT	Control CT
Emphysema (%)	0.1 ± 0.13	0.7 ± 1.2	0.2 ± 0.3	2 ± 3.6
Normal pulmonary parenchyma (%)	35 ± 11.8	65 ± 15 ***	34 ± 13	41 ± 10††
Ground glass opacity (%)	49 ± 11	25 ± 10 ***	46 ± 7	42 ± 6.7††
Consolidation (%)	4.4 ± 2.7	3.3 ± 2.6	5.6 ± 4.6	5 ± 2.9
Other (%)	11 ± 4.5	5 ± 4.5 **	14.8 ± 10.8	11.6 ± 2.9†

(ACE-2) receptor, displaying profound tropism for the human vascular endothelium and the lungs [49,50]. Inflamed endothelial cells induce proinflammatory cytokine production, leading to general hyperinflammation with the subsequent influx of activated monocytes, neutrophils, and other immune cells. An increase in blood neutrophils with a low lymphocyte count may predict poor outcomes. It has been shown that an increase in NLR above 10 is a strong predictor of fatal outcomes in critically ill COVID-19 patients [50,51].

#### 4.3. Endotheliopathy

Severe COVID-19 has been linked to endotheliopathy and vasculitis, which has been documented in several studies [1–4,52,53]. Elevated plasma D-dimer concentrations, which are fibrin degradation fragments, are associated with an increased risk for morbidity and mortality in COVID-19 patients [54,55]. The virus possesses a strong affinity for the vascular endothelium, leading to lymphocytic endotheliitis with infiltration of inflammatory cells around the vessels and endothelial apoptotic cell death [56]. A rapid increase in the concentration of proinflammatory cytokines, such as IL-6 and TNF- $\alpha$ , reduces the physiological antithrombotic and anti-inflammatory functions of endothelial cells and triggers a procoagulopathy cascade [57]. Hence, extensive inflammation may disturb the crosstalk between the endothelium, platelets, and the coagulation system, leading to the formation of clots in the microvascular circulation of several organs, especially the lungs. Xanthohumol inhibits inflammatory-induced endothelial dysregulation, exerting antiangiogenic and anti-inflammatory effects via the reduction of NF- $\kappa$ B activity, a well-established angiogenic and inflammatory factor [39,40,58]. Interestingly, an experimental study documented that Xn at a dose of 10 mg/kg body weight administered twice daily for 7 days improves blood velocity and reduces the risk of arterial thrombosis, decreasing the incidence of pulmonary embolism [59]. Additionally, treatment with Xn does not affect other coagulation factors, such as prothrombin time (PT), activated partial thrombin time (APTT), or thrombin time (TT), but it insignificantly inhibits platelet activation and adhesion on collagen-coated surfaces [59]. In the present study, we noted a much more profound decrease in D-dimers in the Xn group than in the control group. Additionally, changes in lung CT were also more pronounced in the Xn group. Therefore, we can speculate that Xn reduces vascular damage and the formation of microarterial thrombosis; however, this hypothesis should be confirmed in additional studies.

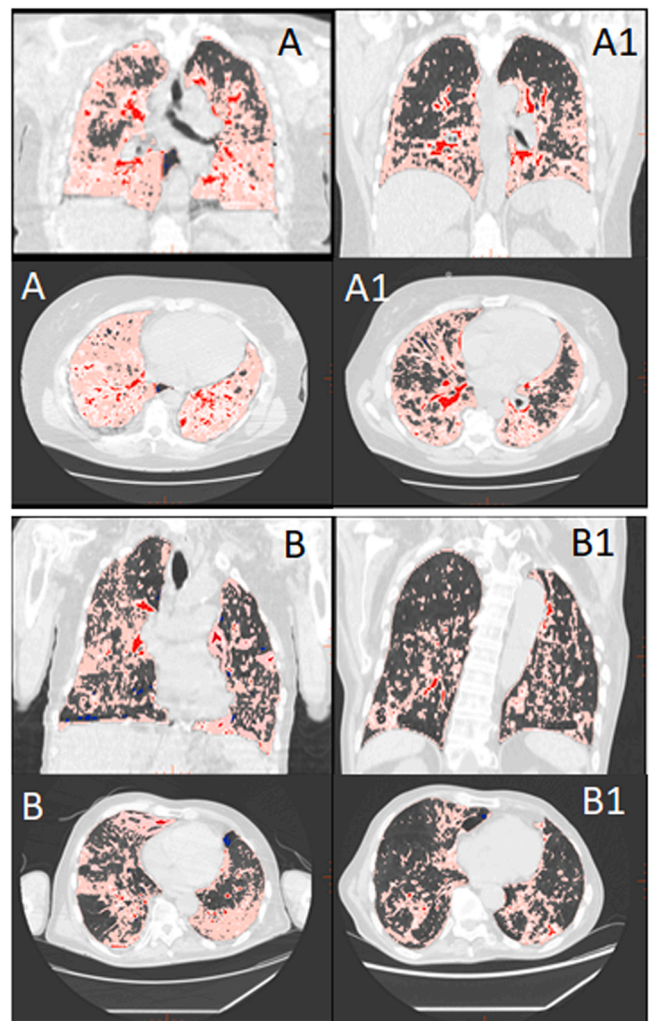


**Fig. 5.** Examples of quantitative computed tomography (CT) of the lung with thoracic VCAR analysis from 2 patients successfully treated with Xn at a daily dose of 4.5 mg/kg body weight for severe COVID-19. Both were mechanically ventilated with  $FO_2$  1.0 in the prone position. Panel A - patient A: CT examination at baseline (A-0) was performed a few hours before the start of mechanical ventilation. The first dose of Xn 1.5 mg/kg body weight (158 mg of Xn) was administered before intubation. The baseline  $PaO_2/FiO_2$  immediately after intubation was 58. After 6 days, the patient was extubated, and a control CT (A-1) was performed on Day 8. His  $PaO_2/FiO_2$  was 232 on the 7th treatment day (end of the study period). This patient was transferred to the pulmonology ward and discharged to home after 32 days of treatment in good clinical condition. Panel B - patient B: CT examination at baseline (B-0) was performed just before admission to the ICU. The first dose of Xn was administered immediately before admission. The patient was intubated within 3 h after admission to the ICU, and mechanical ventilation in the prone position was started after intubation. His baseline  $PaO_2/FiO_2$  was 52 just after intubation. The patient was extubated on the 7th day of treatment, and a control CT (B-1) was performed on the 9th day. The patient was discharged to the pulmonology ward and then discharged to home on Day 35.

#### 4.4. Limitations

Despite its promising findings, our study has several limitations. First, because of the small number of patients treated with Xn, the power of our analysis was significantly reduced. Second, our analysis of Xn-related anti-inflammatory effects was based on only a few commonly assessed variables. Several experimental studies have documented that Xn reduces many circulating proinflammatory cytokines in different diseases [8,23–26,40,60,61]. Third, we did not analyze blood Xn levels

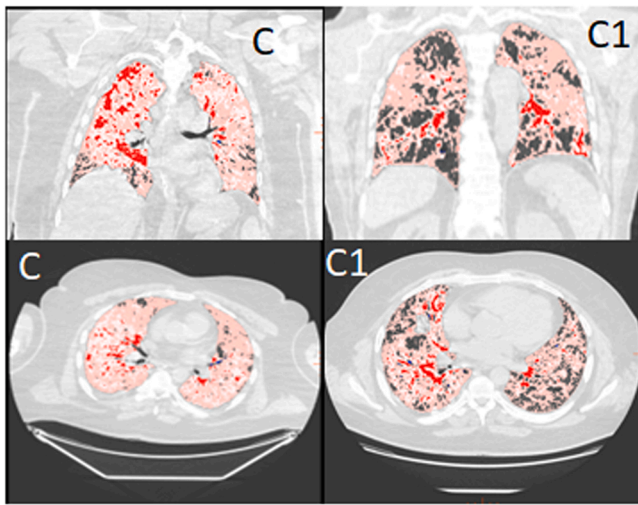


**Fig. 6.** Example of quantitative computed tomography (CT) of the lung with thoracic VCAR analysis in a patient treated with placebo (NaCl 0.9% at a dose of 3 mL administered 3 times per day). The patient was mechanically ventilated with FO<sub>2</sub> 1.0 in the prone position. Quantitative CT was performed a few hours before the start of mechanical ventilation (C). The baseline PaO<sub>2</sub>/FiO<sub>2</sub> just after intubation was 55. After 13 days, the patient was extubated and placed on noninvasive ventilation (NIV). The patient was transferred to another hospital and was finally discharged to home on Day 98.

or its metabolite concentrations. Previous studies have shown that Xn is a safe and nontoxic supplementary product; however, its interaction with other anti-inflammatory medications has not been well documented.

Additionally, we did not analyze the effect of Xn on blood glucose levels. Experimental studies have shown that Xn may be favorable for glucose metabolism, and treatment with Xn at a dose of 60 mg/kg body weight per day effectively reduced plasma glucose, total cholesterol, and LDL-cholesterol concentrations [42,62]. A reduction in plasma glucose concentration following Xn administration was only noted in male mice, whereas higher liver concentrations of Xn and its metabolites were found in female mice [62]. It has been well established that IL-6 affects glucose homeostasis. Increased IL-6 levels impair insulin action, whereas inhibiting IL-6 improves hepatic insulin sensitivity [63,64]. In the present study, the blood glucose concentration was maintained with continuous insulin administration, and the dose of insulin was not analyzed. Therefore, we hypothesize that Xn affects glucose metabolism via a decrease in IL-6 concentration; however, this hypothesis should be confirmed in additional studies.

Fifth, estrogen and other sex hormone activity was not monitored. Importantly, Xn exhibits estrogen activity by increasing the level of 8-prenylnarigenin, which strongly reduces the inflammatory response and proinflammatory cytokine release [62,65,66]. Additionally, 8-prenylnarigenin also shows anti-inflammatory and vascular-protective properties, which could have had a significant impact on our patients [64]. Sex steroids are potent immune modulators and suppress the production of proinflammatory cytokines, such as IL-6, IL-1 $\beta$ , and TNF- $\alpha$  [67]. An experimental study showed a reduction in IL-6 production following estrogen administration, and clinical observations documented a negative correlation between plasma estrogen concentration and lung functionality in COVID-19 patients [68,69]. Another clinical observation documented a significantly increased mortality rate and worse respiratory failure in men relative to women [70]. Estrogen supplementation was also associated with a decreased risk of death in postmenopausal women [71]. In the present study, the numbers of men and women were comparable in the studied groups. However, only one woman died in the Xn group, and two died in the control group. Therefore, we hypothesize that the Xn-related increase in the estrogen

concentration might play a role in the outcome but the limited number of patients and lack of hormone control preclude drawing such a conclusion.

In the present study, we confirmed the beneficial effects of adjuvant therapy with Xn in critically ill COVID-19 patients requiring mechanical ventilation. Based on our findings, we hypothesize that Xn may also improve the clinical course of COVID-19 in patients with only slight symptoms and may reduce the risk of developing severe respiratory failure and the need for mechanical ventilation; however, this hypothesis must be confirmed in additional studies.

## 5. Conclusions

Xanthohumol is a promising adjuvant treatment for COVID-19 patients with severe respiratory failure who require mechanical ventilation. Treatment with Xn improved the clinical course and reduced the severity of the inflammatory response and mortality rate. Additional studies in a large cohort of patients are needed to confirm these findings.

## Funding

This study was supported by a grant from the Medical University of Lublin, Poland (DS 352/2019). The funder had no role in the study design, data collection, analysis, decision to publish, or preparation of the manuscript.

## CRedit authorship contribution statement

Wojciech Dabrowski – conceptualisation, methodology, writing – original draft preparation, software. Mariusz Gagos - conceptualisation, methodology, statistical analysis. Dorota Siwicka-Gieroba – data collection, data interpretation. Mariusz Piechota – data collection, visualization. Jan Siwiec – data collection, data interpretation. Andrzej Stepulak – supervision, writing – original draft preparation. Luiza Grzycka-Kowalczyk – CT scans preparation, data collection. Magdalena Bielacz – writing – original draft preparation, visualization. Katarzyna Kotfis – conceptualisation, methodology, writing – original draft preparation, statistical analysis. Andrzej Jaroszynski – supervision, original draft preparation. Manu LNG Malbrain – conceptualisation, supervision, data analysis, language correction.

## Ethical approval and consent to participate

This study was conducted in accordance with the Declaration of Helsinki and applicable regulatory requirements and was approved by the Institutional Review Board and the Bioethics Committee of the Medical University at Lublin, Poland (KE-0254/201/2020). Informed consent was obtained from all patients. Additionally, their legal representatives were informed about the main purpose of this study.

## Consent for publication

Written informed consent for publication was obtained from all patients.

## Conflict of interests

All authors declare no conflicts of interest. Additionally, none of the authors received money in connection with this research.

## Data Availability

Data will be made available on request.

## References

- [1] M. Yamaoka-Tojo, Endothelial glycoalkal damage as a systemic inflammatory microvascular endotheliopathy in COVID-19, *Biomed. J.* 43 (2020) 399–413, <https://doi.org/10.1016/j.bj.2020.08.007>.
- [2] M. Yamaoka-Tojo, Vascular endothelial glycoalkal damage in COVID-19, *Int J. Mol. Sci.* 21 (2020) 9712, <https://doi.org/10.3390/ijms21249712>.
- [3] Y. Lei, J. Zhang, C.R. Schiavon, M. He, L. Chen, H. Shen, et al., SARS-CoV-2 spike protein impairs endothelial function via downregulation of ACE 2, *Circ. Res* 128 (2021) 1323–1326, <https://doi.org/10.1161/CIRCRESAHA.121.318902>.
- [4] S. Pons, S. Fodil, E. Azoulay, L. Zafrani, The vascular endothelium: the cornerstone of organ dysfunction in severe SARS-CoV-2 infection, *Crit. Care* 24 (2020) 353, <https://doi.org/10.1186/s13054-020-03062-7>.
- [5] S. Hoyo, M. Uchida, K. Tanaka, R. Hasebe, Y. Tanaka, Murakami, et al., How COVID-19 induces cytokine storm with high mortality, *Inflamm. Regen.* 40 (2020) 1–7, <https://doi.org/10.1186/s41232-020-00146-3>.
- [6] J. Zhang, Z. Wang, X. Wang, Z. Hu, C. Yang, P. Lei, Risk factors for mortality of COVID-19 patient based on clinical course: a single centre retrospective case-control study, *Front Immunol.* 12 (2021), 581469, <https://doi.org/10.3389/fimmu.2021.581469>.
- [7] N. Morgulchik, F. Athanasopoulou, E. Chu, Y. Lam, N. Kamaly, Potential therapeutic approaches for targeted inhibition of inflammatory cytokines following COVID-19 infection-induced cytokine storm, *Interface Focus* 12 (2021), 20210006, <https://doi.org/10.1098/rsfs.2021.0006>.
- [8] G. Chen, D. Wu, Y. Cao, D. Huang, H. Wang, T. Wang, et al., Clinical and immunological features of severe and moderate coronavirus disease 2019, *J. Clin. Invest* 130 (2020) 2620–2629, <https://doi.org/10.1172/JCI137244>.
- [9] N. Majidi, F. Rabbani, S. Gholami, M. Gholamalizadeh, F. BourBour, S. Rastgoo, et al., The effect of vitamin C on pathological parameters and survival duration of critically ill coronavirus disease 2019 patients: a randomized clinical trial, *Front Immunol.* 12 (2021), 717816, <https://doi.org/10.3389/fimmu.2021.717816>.
- [10] D. Rawat, A. Roy, S. Maitra, A. Gulati, P. Khanna, D.K. Baidy, Vitamin C and COVID-19 treatment: a systematic review and meta-analysis of randomized controlled trials, *Diabetes Metab. Syndr.* 15 (2021), 102324, <https://doi.org/10.1016/j.dsx.2021.102324>.
- [11] M. Roumier, R. Paule, M. Groh, A. Vallee, F. Ackerman, Interleukin-6 blockade for severe COVID-19, *medRxiv* (2020), <https://doi.org/10.1101/2020042020061861>.
- [12] E.C. Somers, G.A. Eschenauer, J.P. Troost, J.L. Golob, T.N. Gandhi, L. Wang, et al., Tocilizumab for treatment of mechanically ventilated patients with COVID-19, *Clin. Inf. Dis.* 73 (2021) e445–e454, <https://doi.org/10.1101/2020.05.29.20117358>.
- [13] F. Angriani, B.L. Ferreyro, L. Burry, E. Fan, N.D. Ferguson, S. Husain, et al., Interleukin-6 receptor blockade in patients with COVID-19: placing clinical trials into context, *Lancet Resp. Med.* 9 (2021) 655–664, [https://doi.org/10.1016/S2213-2600\(21\)00139-9](https://doi.org/10.1016/S2213-2600(21)00139-9).
- [14] M. Shohan, R. Nashibi, M.R. Mahmoudian-Sani, F. Abolnezhadian, M. Ghafourian, S.M. Alavi, et al., The therapeutic efficacy of quercetin in combination with antiviral drugs in hospitalized COVID-19 patients: a randomized controlled trial, *Eur. J. Pharmacol.* 914 (2022), 174615, <https://doi.org/10.1016/j.ejphar.2021.174615>.
- [15] A. Malik, A. Naz, S. Ahmad, M. Hafeez, F.M. Awan, T.H. Jafar, et al., Inhibitory potential of phytochemicals on interleukine-6 mediated T-cells reduction in COVID-19 patients: a computational approach, 11779322211021430, *Bioinform. Biol. Insights* 15 (2021), <https://doi.org/10.1177/11779322211021430>.
- [16] A.F. De Melo, M. Homem-de-Mello, High-dose intravenous vitamin C may help in cytokine storm in severe SARS-CoV-2 infection, *Crit. Care* 24 (1) (2020) 500, <https://doi.org/10.1186/s13054-020-03228-3>.
- [17] K. Al Sulaiman, O. Aljuhani, Al, A.I. Shaya, A. Kharbosh, R. Kearsara, A. Al Guwairy, et al., Evaluation of zinc sulfate as an adjunctive therapy in COVID-19 critically ill patients: a two center propensity-score matched study, *Crit. Care* 25 (1) (2021) 363, <https://doi.org/10.1186/s13054-021-03785-1>.
- [18] M.M. Ngwe Tun, K. Toume, E. Luvai, K.M. New, S. Mizukami, K. Hirayama, et al., The discovery of herbal drugs and natural compounds as inhibitors of SARS-CoV-2 infection in vitro, *J. Nat. Med.* 10 (2022) 1–8, <https://doi.org/10.1007/s11418-021-01596-w>.
- [19] M. Shohan, R. Nashibi, M.R. Mahmoudian-Sani, F. Abolnezhadian, M. Ghafourian, S.M. Alavi, et al., The therapeutic efficacy of quercetin in combination with antiviral drugs in hospitalized COVID-19 patients: a randomized control trial, *Eur. J. Pharmacol.* 914 (2022), 174615, <https://doi.org/10.1016/j.ejphar.2021.174615>.
- [20] S. Yuan, B. Yan, J. Cao, Z.W. Ye, R. Liang, K. Tang, et al., SARS-CoV-3 exploits host DGAT and ADRP for efficient replication, *Cell Disco* 7 (2021) 100, <https://doi.org/10.1038/s41421-021-00338-2>.
- [21] M. Russo, S. Moccia, C. Spagnuolo, I. Tedesco, G.L. Russo, Roles of flavonoids against coronavirus infection, *Chem. Biol. Inter.* 328 (2020), 109211, <https://doi.org/10.1016/j.cbi.2020.109211>.
- [22] M.R. Peluso, C.L. Miranda, D.J. Hobbs, R.P. Proteau, J.F. Stevens, Xanthohumol and related prenylated flavonoids inhibit inflammatory cytokine production in LPS-activated THP-1 monocytes: structure-activity relationships and in silico binding to myeloid differentiation protein-2 (MD-2), *Planta Med* 76 (2010) 1536–1543, <https://doi.org/10.1055/s-0029-1241013>.
- [23] D. Elkhalfi, I. Al-Hashimi, A.E. Al Moustafa, A. Khalil, A comprehensive review on the antiviral activities of chalcones, *J. Drug Target* 29 (2021) 403–419, <https://doi.org/10.1080/1061186X.2020.1853759>.
- [24] X. Gao, D. Deeb, Y. Liu, S. Gautam, S.A. Dulchavsky, S.C. Gautam, Immunomodulatory activity of Xanthohumol: inhibition of T cell proliferation, cell-mediated cytotoxicity and Th1 cytokine production through suppression of NF-kappaB, *Immunopharmacol. Immunotoxicol.* 31 (2009) 477–484, <https://doi.org/10.1080/08923970902798132>.
- [25] S. Luescher, C. Urmann, V. Butterweck, Effect of Hops derived prenylated phenols on TNF- $\alpha$  induced barrier dysfunction in intestinal epithelial cells, *J. Nat. Prod.* 80 (2017) 925–931, <https://doi.org/10.1021/acs.jnatprod.6b00869>.
- [26] G.I. Vazquez-Cervantes, D.R. Ortega, T. Blanco Ayala, V. Pérez de la Cruz, D.F. G. Esquivel, A. Salazar, B. Pineda, Redox and anti-inflammatory properties from Hop components in beer-related to neuroprotection, *Nutrients* 13 (2021) 2000, <https://doi.org/10.3390/nu13062000>.
- [27] X. Liu, J. Bai, C. Jiang, Z. Song, Y. Zhao, H. Nauwynck, P. Jiang, Therapeutic effect of Xanthohumol against highly pathogenic porcine reproductive and respiratory syndrome viruses, *Vet. Microbiol.* 238 (2019), 108431, <https://doi.org/10.1016/j.vetmic.2019.108431>.
- [28] X. Liu, Z. Song, J. Bai, H. Nauwynck, Y. Zhao, P. Jiang, Xanthohumol inhibits PRRSV proliferation and alleviates oxidative stress induces by PRRSV via the Nrf2-HMOX1 axis, *Vet. Res.* 50 (2019) 61, <https://doi.org/10.1016/j.vetmic.2019.108431>.
- [29] Y. Lin, R. Zhang, Y. Ma, Z. Wang, S. Ding, R. Zhang, et al., Xanthohumol is a potent pan-inhibitor of coronaviruses targeting main protease, *Int J. Mol. Sci.* 22 (2021) 12134, <https://doi.org/10.3390/ijms222212134>.
- [30] L. Legette, C. Karnpracha, R.L. Reed, J. Choi, G. Bobe, J.M. Christensen, et al., Human pharmacokinetics of Xanthohumol and antihyperglycemic flavonoid from hops, *Mol. Nutr. Food Res.* 58 (2014) 248–255, <https://doi.org/10.1002/mnfr.201300333>.
- [31] W. Dabrowski, D. Siwicka-Gieroba, C. Robba, R. Badenes, M.L.N.G. Malbrain, The prone position must accommodate in IAP in traumatic brain injury patients, *Crit. Care* 25 (2021) 132, <https://doi.org/10.1186/s13054-021-03506-8>.
- [32] R. Zahorec, Neutrophil-to-lymphocyte ratio, past, present and future perspective, *Bratisl. Lek. Listy* 122 (2021) 474–488, <https://doi.org/10.4149/BLL-2021-078>.
- [33] A.P. Yang, J.P. Liu, W.Q. Tao, H.M. Li, The diagnostic and predictive role of NLR, d-NLR and PLR in COVID-19 patients, *Int Immunopharmacol.* 84 (2020), 106504, <https://doi.org/10.1016/j.intimp.2020.106404>.
- [34] J.F. Stevens, A.W. Taylor, J.E. Clawson, M.L. Deinzer, Fate of Xanthohumol and related preflavonoids from hop to beer (doi.org/), *J. Agric. Food Chem.* 47 (1999) 2421–2428, <https://doi.org/10.1021/jf990101k>.
- [35] D. Nikolic, Y. Li, L.R. Chadwick, G.F. Pauli, R.B. van Breemen, Metabolism of Xanthohumol and isoxanthohumol, prenylated flavonoids from hops (*Humulus lupulus* L.) by human liver microsomes, *J. Mass Spectrom.* 40 (2005) 289–299, <https://doi.org/10.1002/jms.753>.
- [36] M. Yilmazer, J.F. Stevens, D.R. Buhler, In vitro glucuronidation of Xanthohumol, a flavonoid in hop and beer, by rat and human liver microsomes, *FEBS Lett.* 491 (2001) 252–256, [https://doi.org/10.1016/S0014-5793\(01\)02210-4](https://doi.org/10.1016/S0014-5793(01)02210-4).
- [37] S. Shiwakoti, D. Adhikari, J.P. Lee, K.W. Kang, I.S. Lee, H.J. Kim, M.H. Oak, Prevention of fine dust-induced vascular senescence by Humulus lupulus extract and its major bioactive compounds, *Antioxidants* 9 (2020) 1243, <https://doi.org/10.3390/antiox9121243>.
- [38] N. Zhang, B. Tian, S. Zhao, X. Zhang, D. Pan, X. Shen, Y. Zhang, A new formylated chalcone from Humulus lupulus with protective effect on HUVECs injury by angiotensin II, *Nat. Prod. Res* 33 (2019) 617–621, <https://doi.org/10.1080/14786419.2017.1402318>.
- [39] C. Gallo, K. Dallaglio, T. Bassani, T. Rossi, A. Rosello, D.M. Noonan, G. D’Uva, A. Bruno, A. Albin, Hop derived flavonoid xanthohumol inhibits endothelial cell functions via AMPK activation, *Oncotarget* 7 (2016) 59917–59931, <https://doi.org/10.18632/oncotarget.10990>.
- [40] H. Lv, Q. Liu, Z. Wen, H. Feng, X. Deng, X. Ci, Xanthohumol ameliorates lipopolysaccharide (LPS)-induces acute lung injury via induction of AMPK/GSK3 $\beta$ -Nef2 signal axis, *Redox Biol.* 12 (2017) 311–324, <https://doi.org/10.1016/j.redox.2017.03.001>.
- [41] M.T. Khayyal, R.M. El-Hazek, W.A. El-Sabbagh, J. Frank, D. Behnam, M. Abdel-Tawab, Micellar solubilization enhances the anti-inflammatory effect of Xanthohumol, *Phytomedicine* 71 (2020), 153233, <https://doi.org/10.1016/j.phymed.2020.153233>.
- [42] C.L. Miranda, V.D. Elias, J.J. Hay, J. Choi, R.D. Reed, J.F. Stevens, Xanthohumol improves dysfunctional glucose and lipid metabolism in diet-induced obese C57BL/6J mice, *Arch. Biochem. Biophys.* 599 (2016) 22–30, <https://doi.org/10.1016/j.abb.2016.03.008>.
- [43] D. Siwicka-Gieroba, K. Malodobry, J. Biernawska, C. Robba, R. Bohatyrewicz, R. Rola, W. Dabrowski, The neutrophil/lymphocyte count ratio predicts mortality in severe traumatic brain injury patients, *J. Clin. Med.* 8 (2019) 1453, <https://doi.org/10.3390/jcm8091453>.
- [44] R. Aktimur, S. Cetinkunar, K. Yildirim, S.H. Aktimur, M. Ugurlucan, N. Ozlem, Neutrophil-to-lymphocyte ratio as a diagnostic biomarker for the diagnosis of acute mesenteric ischemia, *Eur. J. Trauma Emerg. Surg.* 42 (2016) 363–368, <https://doi.org/10.1007/s00068-015-0546-4>.
- [45] Z. Huang, Z. Fu, W. Huang, K. Huang, Prognostic value of neutrophil-to-lymphocyte ratio in sepsis: a meta-analysis, *Am. J. Emerg. Med* 38 (2020) 641–647, <https://doi.org/10.1016/j.ajem.2019.10.023>.
- [46] S. Jimeno, P.S. Ventura, J.M. Castellano, S.I. Garcia-Adasme, M. Miranda, P. Touza, et al., Prognostic implication of neutrophil-lymphocyte ratio in COVID-19, *Eur. J. Clin. Invest.* 51 (2021), e13404, <https://doi.org/10.1111/eci.13404>.
- [47] D.M. Mizurini, E.D. Hottz, P.T. Bozza, R.Q. Monteiro, Fundamentals in COVID-19 – associated thrombosis: molecular and cellular aspects, *Front Cardiovasc Med* 8 (2021), 785738, <https://doi.org/10.3389/fcvm.2021.785738>.

- [48] M. Leppkes, J. Knopf, E. Naschberger, A. Lindemann, J. Singh, I. Herrmann, et al., Vascular occlusion by neutrophil extracellular traps in COVID-19, *EBioMedicine* 58 (2020), 102925, <https://doi.org/10.1016/j.ebiom.2020.102925>.
- [49] L. Schimmel, K.Y. Chew, C.J. Stocks, T.E. Yordanov, P. Essebier, A. Kulasinghe, et al., Endothelial cells are not productively infected by SARS-CoV-2, *Clin. Transl. Immunol.* 10 (2021), e1350, <https://doi.org/10.1002/cti2.1350>.
- [50] Z. Verga, A.J. Flammer, P. Steiger, M. Haberecker, R. Andermatt, A.S. Zinkernagel, M.R. Mehra, et al., Endothelial cell infection and endotheliitis in COVID-19, *Lancet* 395 (2020) 1417–1418, [https://doi.org/10.1016/S0140-6736\(20\)30937-5](https://doi.org/10.1016/S0140-6736(20)30937-5).
- [51] P.O.C. Terra, C.D. Donadel, L.C. Oliveira, M.G. Meneguatti, M. Auxiliadora-Martins, R.T. Calado, G.C. De Santis, Neutrophil-to-lymphocyte ratio and D-dimer are biomarkers of death risk in severe COVID-19. A retrospective observational study, *Health Sci. Rep.* 5 (2022), e514, <https://doi.org/10.1002/hsr2.514>.
- [52] T. Ito, M. Kakuuchi, I. Maruyama, Endotheliopathy in septic conditions: mechanistic insight into intravascular coagulation, *Crit. Care* 25 (1) (2021) 95, <https://doi.org/10.1186/s13054-021-03524-6>.
- [53] G. Goshua, A.B. Pine, M.L. Meizlish, C.H. Chang, H. Zhang, P. Bahel, et al., Endotheliopathy in COVID-19-associated coagulopathy: evidence from a single-centre. Cross-sectional study, *Lancet Haematol.* 7 (8) (2020) e575–e582, [https://doi.org/10.1016/S2352-3026\(20\)30216-7](https://doi.org/10.1016/S2352-3026(20)30216-7).
- [54] F. Zhou, T. Yu, R. Du, G. Fan, Y. Liu, Z. Liu, et al., Clinical course and risk factors for mortality of adult inpatients with COVID-19 in Wuhan, China: a retrospective cohort study, *Lancet* 395 (10229) (2020) 1054–1062, [https://doi.org/10.1016/S0140-6736\(20\)30566-3](https://doi.org/10.1016/S0140-6736(20)30566-3).
- [55] J. Xu, X. Yang, L. Yang, Y. Wang, Y. Wu, T. Zhou, et al., Clinical course and predictors of 60-day mortality in 239 critically ill patients with COVID-19: a multicentre retrospective study from Wuhan, China, *Crit. Care* 24 (1) (2020) 394, <https://doi.org/10.1186/s13054-020-03098-9>.
- [56] Z., L.F. Qin, R. Blair, C. Wang, H. Yang, J. Mudd, J.M. Currey, et al., Endothelial cell infection and dysfunction, immune activation in severe COVID-19, *Theranostics* 11 (16) (2021) 8076–8091, <https://doi.org/10.7150/thno.61810>.
- [57] J. Zhang, K.M. Tecson, P.A. McCullough, Endothelial dysfunction contributes to COVID-19-associated vascular inflammation and coagulopathy, *Rev. Cardiovasc. Med.* 21 (3) (2020) 315–319, <https://doi.org/10.31083/j.rcm.2020.03.126>.
- [58] R. Negrao, R. Costa, D. Duarte, T.T. Gomez, M. Mendanha, L. Moura, et al., Angiogenesis and inflammation signalling are targets of beer polyphenols in vascular cells, *J. Cell Biochem.* 111 (2010) 1270–1279, <https://doi.org/10.1002/jcb.22850>.
- [59] G. Xin, Z. Wei, C. Ji, H. Zheng, J. Gu, L. Ma, et al., Xanthohumol isolated from *Humulus lupulus* prevent thrombosis without increased bleeding risk by inhibiting platelet activation and mtDNA release, *Free Radic. Biol. Med.* 108 (2017) 247–257, <https://doi.org/10.1016/j.freeradbiomed.2017.02.018>.
- [60] M.P. Pluta, M.N. Zachura, K. Winiarska, A. Kalembe, C. Kaplan, A.J. Szczepańska, Ł.J. Krzych, Usefulness of selected peripheral blood counts in predicting death in patients with severe and critical COVID-19, *J. Clin. Med.* 11 (2022) 1011, <https://doi.org/10.3390/jcm11041011>.
- [61] J.M. Cho, S.M. Yun, Y.H. Choi, J. Heo, N.J. Kim, S.H. Kim, E.H. Kim, Xanthohumol prevents dextran sulphate sodium-induced colitis via inhibition of IKK $\beta$ /NF- $\kappa$ B signalling in mice, *Oncotarget* 9 (2018) 866–880, <https://doi.org/10.18632/oncotarget.23183>.
- [62] L.I. Legette, A.Y. Luna, R.L. Reed, C.L. Miranda, G. Bobe, R.R. Proteau, J.F. Stevens, Xanthohumol lowers body weight and fasting plasma glucose in obese male Zucker fa/fa rats, *Phytochemistry* 91 (2013) 236–241, <https://doi.org/10.1016/j.phytochem.2012.04.018>.
- [63] H.J. Kim, T. Higashimori, S.Y. Park, H. Choi, J. Dong, Y.J. Kim, et al., Differential effect of interleukin-6 and -10 on skeletal muscle and liver insulin action in vivo, *Diabetes* 53 (2004) 1060–1067, <https://doi.org/10.2337/diabetes.53.4.1060>.
- [64] D. Cai, M. Yuan, D.F. Frants, P.A. Melendez, L. Hansen, J. Lee, S.E. Shoelson, Local and systemic insulin resistance resulting from hepatic activation of IKK- $\beta$  and NF- $\kappa$ B, *Nat. Med.* 11 (2005) 183–190, <https://doi.org/10.1038/nm1166>.
- [65] S.R. Milligan, J.C. Kalita, V. Pocock, V. Van De Kauter, J.F. Stevens, M.L. Deinzer, et al., The endocrine activities of 8-prenylarigenin and related hop (*Humulus lupulus* L.) flavonoids, *J. Clin. Endocrinol. Metab.* 85 (2000) 4912–4915, <https://doi.org/10.1210/jcem.85.12.7168>.
- [66] T. Paoletti, S. Fallarini, F. Gugliesi, A. Minassi, G. Appendino, G. Lombardi, Anti-inflammatory and vascular protective properties of 8-prenylapigenin, *Eur. J. Pharm.* 620 (2009) 120–130, <https://doi.org/10.1016/j.ejphar.2009.08.015>.
- [67] R.H. Straub, The complex role of estrogens in inflammation, *Endocr. Rev.* 28 (2007) 521–574, <https://doi.org/10.1210/er.2007-0001>.
- [68] J.Y. Youn, Y. Zhang, Y. Wu, M. Cannesson, H. Cai, Therapeutic application of estrogen for COVID-19: attenuation of SARS-CoV-2 spike protein and IL-6 stimulated, ACE2-dependent NOX2 activation, ROS production and MCP-1 upregulation in endothelial cells, *Redox Biol.* 46 (2021), 102099, <https://doi.org/10.1016/j.redox.2021.102099>.
- [69] M.T. Pagano, D. Peruzzi, L. Busani, M. Pierdominici, A. Ruggieri, A. Antinori, et al., Predicting respiratory failure in patients infected by SARS-CoV-2 by admission sex-specific biomarkers, *Biol. Sex. Differ.* 12 (2021) 63, <https://doi.org/10.1186/s13293-021-00407-x>.
- [70] S.S. Bhopal, R. Bhopal, Sex differential in COVID-19 mortality varies markedly by age, *Lancet* 396 (2020) 532–533, [https://doi.org/10.1016/S0140-6736\(20\)31748-7](https://doi.org/10.1016/S0140-6736(20)31748-7).
- [71] M. Sound, O. Fonseca-Rodriguez, A. Josefsson, K. Welen, A.M. Fors Connolly, Association between pharmaceutical modulation of oestrogen in postmenopausal women in Sweden and death due to COVID-19: a cohort study, *BMJ Open* 12 (2022), e053032, <https://doi.org/10.1136/bmjopen-2021-053032>.